Hindawi Publishing Corporation
Journal of Nanomaterials
Volume 2015, Article ID 584320, 7 pages
http://dx.doi.org/10.1155/2015/584320

Research Article

Room Temperature Imprint Using Crack-Free Monolithic SiO_2-PVA Nanocomposite for Fabricating Microhole Array on Silica Glass

Shigeru Fujino and Hiroshi Ikeda

Art, Science and Technology Center for Cooperative Research, Kyushu University, Kasuga-shi, Fukuoka 816-8580, Japan

Correspondence should be addressed to Shigeru Fujino; fujino@astec.kyushu-u.ac.jp

Received 12 June 2015; Accepted 11 August 2015

Academic Editor: Nandi Zhou

This paper aims to fabricate microhole arrays onto a silica glass via a room temperature imprint and subsequent sintering by using a monolithic SiO_2-poly(vinyl alcohol) (PVA) nanocomposite as the silica glass precursor. The SiO_2-PVA suspension was prepared from fumed silica particles and PVA, followed by drying to obtain tailored SiO_2-PVA nanocomposites. The dependence of particle size of the fumed silica particles on pore size of the nanocomposite was examined. Nanocomposites prepared from 7 nm silica particles possessed suitable mesopores, whereas the corresponding nanocomposites prepared from 30 nm silica particles hardly possessed mesopores. The pore size of the nanocomposites increased as a function of decreasing pH of the SiO_2-PVA suspension. As a consequence, the crack-free monolithic SiO_2-PVA nanocomposite was obtained using 7 nm silica particles via the suspension at pH 3. Micropatterns were imprinted on the monolithic SiO_2-PVA nanocomposite at room temperature. The imprinted nanocomposite was sintered to a transparent silica glass at 1200°C in air. The fabricated sintered glass possessed the microhole array on their surface with aspect ratios identical to the mold.

1. Introduction

Glass imprint processes have attracted interest for commercial manufacture of micro- or nanostructures for optics, electrics, and biodevices, for example, microlens arrays [1, 2], surface-relief gratings [3], infrared polarizers [4], antireflective lenses [5], optical waveguides [6], and microfluidic chips [7, 8]. Recently there has been ever-increasing interest in the research of microperiodic structure fabrication with high aspect ratios. However, there are few reports applying glass imprint methodologies to industrial manufacturing processes. One significant challenge for the success of glass imprinting is the durability of the mold at high temperatures. To avoid degradation of the imprint mold, considerable effort has been paid to develop low-softening-temperature glasses [9–11]. Conversely, silica glass has been applied to many industrial fields resulting from excellent thermal, chemical, mechanical, and optical properties. There has been a wealth of research into the fabrication of micro- or nanostructures on silica glasses. Owing to a rather high softening temperature, thermal imprinting for silica glass has been performed above 1300°C [12]. To avoid chemical reaction between silica glass and the imprint mold at high temperature, a glassy carbon was chosen as the mold material. However, as the glassy carbon is brittle, decomposition during the imprint at high temperature resulted. Therefore, a further challenge is required to address repeated imprint for the silica glass.

Recently, we developed an alternative and new type of imprint process for silica glass at low temperatures [13]. Figure 1 schematically represents a flowchart of the developed imprint process using a porous SiO_2-PVA nanocomposite as a glass precursor. Firstly, the porous SiO_2-PVA nanocomposite was prepared from silica nanoparticles and poly(vinyl alcohol) (PVA) via a suspension. Thereafter, the imprint was performed at room temperature. The nanocomposite exhibits plastic deformation even at room temperature, which enables transferring of the patterns from the mold to the nanocomposite. Finally, the imprinted nanocomposite was sintered

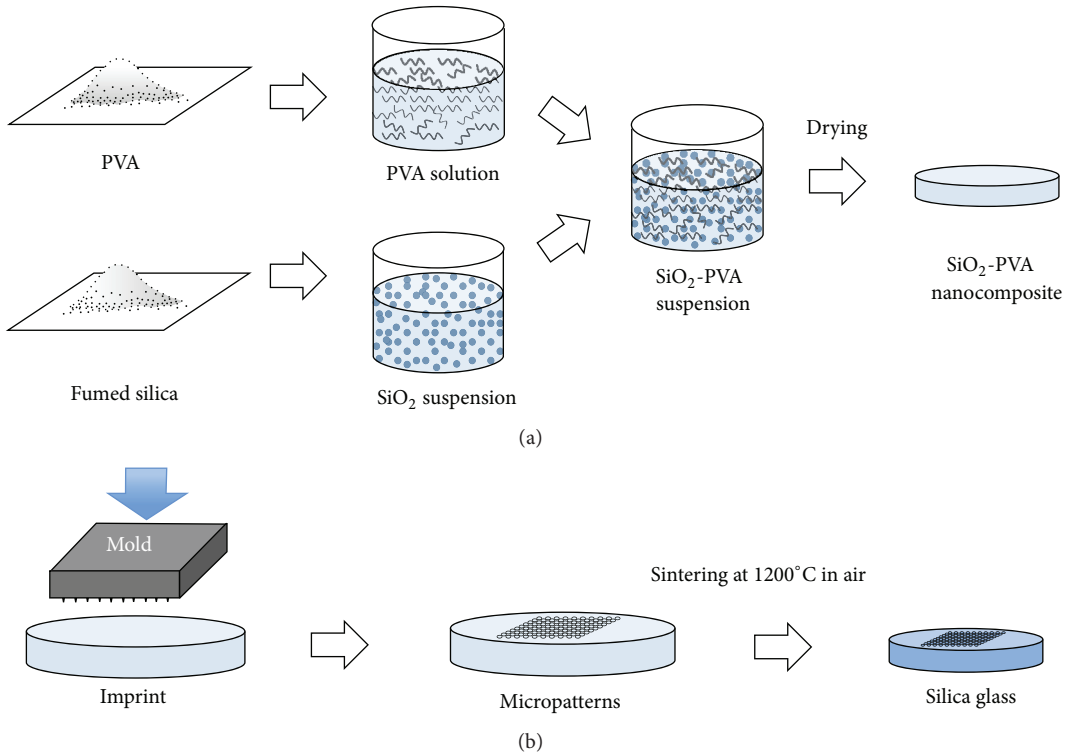

Figure 1: Flowchart for (a) the preparation process of the monolithic SiO_2-PVA nanocomposites and (b) the fabrication process of the micropatterns on the silica glass by room temperature imprint using monolithic SiO_2-PVA nanocomposites as silica glass precursors via the sintering.

to form silica glass. The previous researches have shown holes and lines of submicrometer dimensions successfully fabricated onto the silica glass by this process [13].

In this study, we further performed the room temperature imprint using the SiO_2-PVA nanocomposite to fabricate a series of complicated micropatterns on the silica glass. To perform the room temperature imprint, preparing the monolithic SiO_2-PVA nanocomposite is a prerequisite to the silica glass precursor. However, occasionally there is the presence of cracks on the porous nanocomposite during the drying process from the SiO_2-PVA suspension as capillary force arises owing to the surface tension in the pores. To avoid crack generation during drying, the nanocomposite pore size must be strictly controlled. Studies herein examined the effect of the silica particle size on the textural properties of the nanocomposite, so as to fabricate the monolithic nanocomposite in the absence of cracks.

2. Materials and Methods

2.1. Preparation and Characterization of Porous SiO_2-PVA Nanocomposite. The SiO_2-PVA nanocomposite (SiO_2 : PVA = 80 : 20, wt.%) was prepared from PVA and fumed silica particles. Two types of fumed silica particles were supplied by Nippon Aerosil: Aerosil 300 and Aerosil 50, having mean diameters of 7 and 30 nm, respectively. The PVA with degree of PVA polymerization 1500–1800 and hydrolysis 78–82 mol% (Wako Pure Chemical) was used in this study. Each type of fumed silica (2.56 g) was dispersed in 29.44 mL of distilled water by ultrasonication for 1 h at room temperature. The resulting SiO_2 suspension was adjusted to a given pH value using either nitric acid or ammonia accordingly. Separately, PVA (0.64 g) was added to 7.36 mL of distilled water and magnetically stirred at room temperature to prepare the desired PVA solution. The SiO_2 suspension and the PVA solution were mixed homogeneously at room temperature for 12 h; subsequently an SiO_2-PVA suspension was obtained. The SiO_2-PVA suspension was poured into a Teflon container and later dried in an oven at 30°C for 7 days under atmospheric pressure. The SiO_2-PVA nanocomposite product was obtained.

Nitrogen adsorption/desorption isotherms of the SiO_2-PVA nanocomposites were measured using a BELSORP-mini instrument (BEL Japan). Pore size distribution curves for the samples were obtained via the Barrett-Joyner-Halenda (BJH) model [14]. Specific surface areas of the samples were calculated via the Brunauer-Emmett-Teller (BET) model [15].

2.2. Fabrication of Micropatterns on Silica Glass by Room Temperature Imprint. Prior to conducting the room temperature imprint, the prepared SiO_2-PVA nanocomposite was polished using commercial abrasives to flatten the surface. The micropatterned mold was imprinted onto the nanocomposite by means of a press machine (C. Press-0823, Shinko Sellbic, Japan) subjecting the nanocomposite to 200–1500 kg for 2 min at room temperature. Figure 2 depicts the imprint

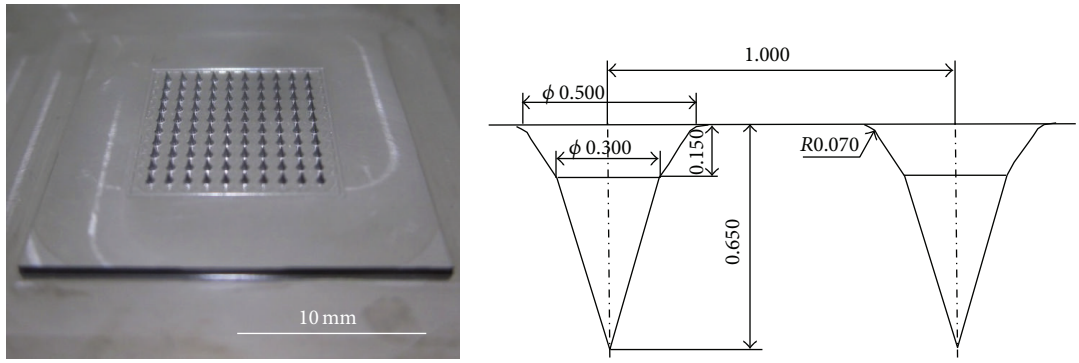

(a) (b)

Figure 2: (a) Photograph of the imprinting mold used in this study and (b) dimensions of the micropillar on the mold.

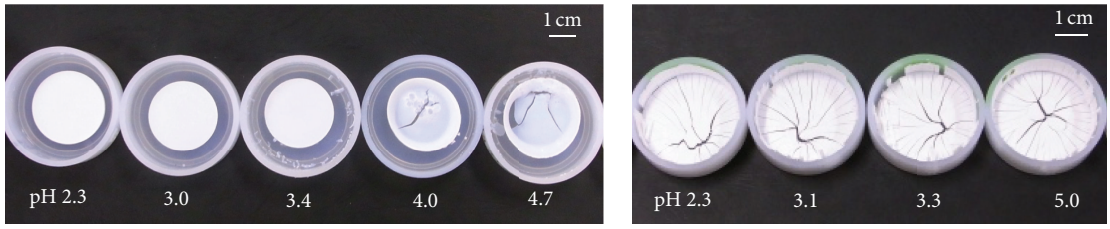

(a) (b)

Figure 3: Photograph of the SiO_2-PVA nanocomposites in the Teflon container after the drying process, (a) prepared from 7 nm and (b) 30 nm silica particles from suspensions with varying pH. The samples at pH 2.3, 3.0, and 3.4 (a) were monolithic and crack-free.

mold used in this study. The imprinting mold has a conical pillar array on the surface. After pressing, the imprinted SiO_2-PVA nanocomposite was calcined at 600°C for 3 h to combust PVA and subsequently sintered at 1200°C for 20 min in air with a heating rate of $5°C \cdot min^{-1}$ to obtain the silica glass. The fabricated patterns on the nanocomposite and sintered samples were observed by a confocal laser scanning microscopy (VK-X210, Keyence, Japan).

3. Results and Discussion

3.1. Crack-Free Monolithic SiO_2-PVA Nanocomposite. Monolithic SiO_2-PVA nanocomposites are required to be further used as silica glass precursors for the room temperature imprint. Therefore, we considered experimental parameters for fabricating a crack-free monolithic SiO_2-PVA nanocomposite, focusing on the silica particle size and pH of the suspension. Figure 3 displays photographs of the as-prepared nanocomposites as a function of particle size and pH. With nanocomposites prepared from 7 nm silica particles, it was evident that no macrocracks were observed for the samples below pH 4. In contrast, for nanocomposites prepared from 30 nm silica particles, an abundance of cracks were observed for all samples, irrespective of the pH value in the examined range.

A previous study reported some crack formation attributed to the capillary force of the solvent within the pores during drying of the suspension forming the porous nanocomposite [16]. Generally, capillary force is considered to depend strongly on the pore size of a porous material. To examine the relationship between pore size of the SiO_2-PVA nanocomposite and crack formation, we evaluated the porous structures of the prepared SiO_2-PVA nanocomposites. Figure 4 presents the pore size distribution of the SiO_2-PVA nanocomposites prepared from 7 and 30 nm silica particles with variation of pH. It was clearly observed that the pore size distribution of the nanocomposites was influenced by the silica particle size. For the nanocomposites prepared from 7 nm silica particles (Figure 4(a)), the pore size exhibited a range of 5–20 nm. In contrast, for the nanocomposite prepared from 30 nm silica particles (Figure 4(b)), the materials hardly possessed pores in the examined range. The results suggested that mesoporous nanocomposites were fabricated by using 7 nm silica particles only. Furthermore, the pore size distribution of the SiO_2-PVA nanocomposites depends on the pH of the SiO_2-PVA suspension, which gradually shift to a decrease in diameter upon increasing the pH. This trend was only observed for the nanocomposites prepared from 7 nm silica particles. According to the previous study on the pH dependence of the pore size of SiO_2-PVA nanocomposites, the pH of the suspension affects the quantity of adsorbed PVA onto the SiO_2 particles, resulting in changes to the pore size distribution [16].

A similar trend to the changes in pore size distribution is also observed on the surface area and pore volume when varying the silica particle size. Table 1 summarizes the textural properties of the nanocomposites. The BET surface areas and pore volumes for the nanocomposites prepared from 7 nm

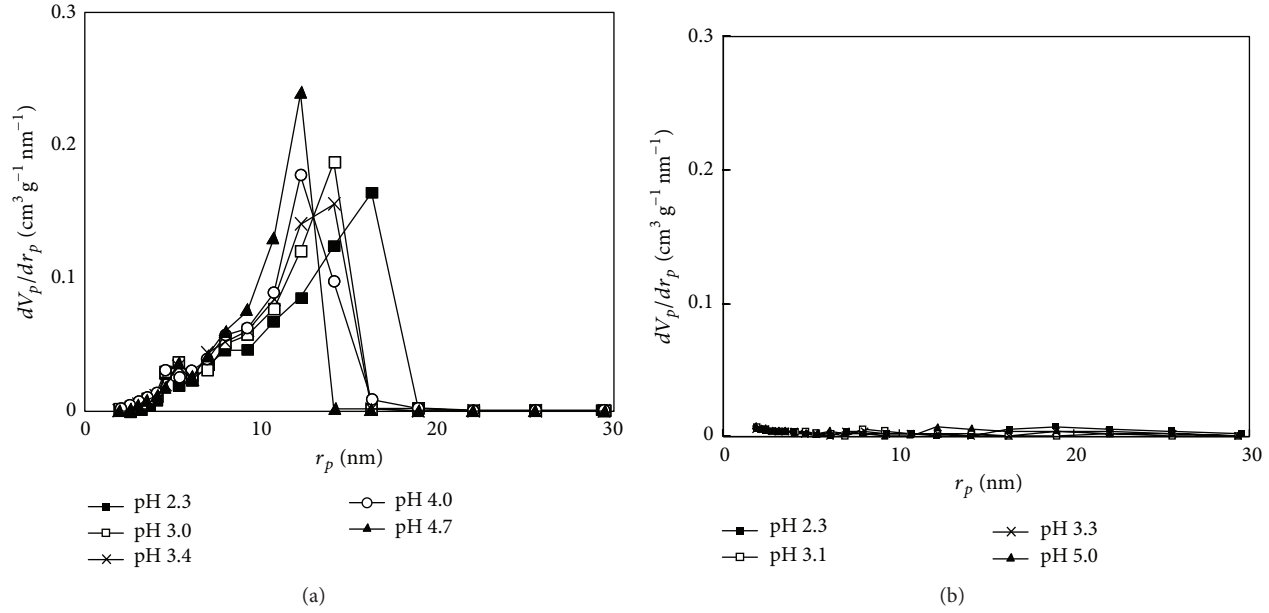

FIGURE 4: Pore size distribution curves of the SiO_2-PVA nanocomposites prepared from (a) 7 nm and (b) 30 nm fumed silica as a function of pH, obtained by means of the BJH method using nitrogen desorption data. "r_p" in the figures indicates radius of the pore.

silica particles were much higher than corresponding values for nanocomposites prepared from 30 nm silica particles.

We discuss below how crack formation is affected as a function of particle size and pH during the drying process with respect to the capillary force on the mesopores. During drying of the porous materials, the capillary force, P, is generated in the material owing to the surface tension of a solvent residing in the pores, expressed as the following equation [17]:

$$P = \frac{2\gamma \cos\theta}{r}, \quad (1)$$

where r is the pore radius, γ is the surface tension of the solvent, and θ is contact angle between the material and the solvent. If the capillary force during drying overcomes the mechanical strength of the porous material, cracks have the potential to form. Thus, to prevent crack formation during drying, there is a preference for the materials to possess large pore sizes. Figure 5 shows the mean pore size of the nanocomposites obtained by the BJH model. The pore size of the nanocomposites prepared from 7 nm silica particles was relatively larger than the corresponding nanocomposites obtained from 30 nm silica particles. Furthermore, the pore size of the nanocomposites increased with decreasing pH. Consequently, the relatively large pores were formed in nanocomposites prepared from 7 nm silica particles with the suspension below pH 4—such material therefore suppresses crack formation as small capillary forces exist during drying.

From these results, mesoporous SiO_2-PVA nanocomposites obtained by using 7 nm silica particles at pH 3 provided optimal prerequisite conditions for use as crack-free nanocomposites for the formation of silica glasses.

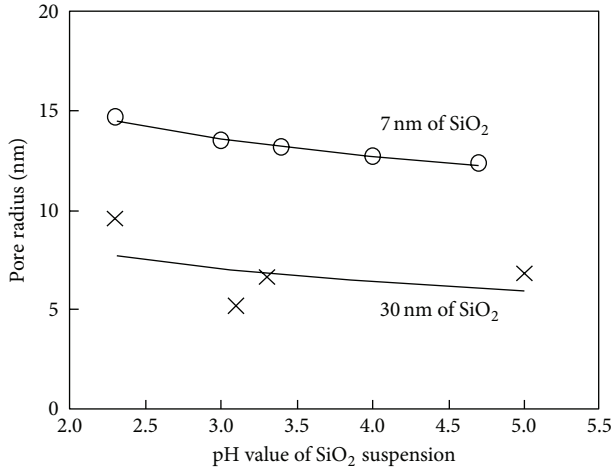

FIGURE 5: Mean pore radius of the SiO_2-PVA nanocomposites prepared from 7 nm and 30 nm silica particles as a function of pH.

3.2. Fabrication of Microhole Array on Sintered Silica Glass via Room Temperature Imprint. Monolithic and crack-free SiO_2-PVA nanocomposite, prepared from 7 nm silica particles within a suspension at pH 3, was used as the silica glass precursor. The imprint was performed at room temperature using the micropatterned mold with variation of the load. Figure 6 shows the profile of the micropattern for the imprinted nanocomposites along with a comparative imprinting mold profile. It appears that conical holes were formed on the SiO_2-PVA nanocomposites by the room temperature imprint. The fabricated shape was near identical to the master shape of the imprinting mold. The result implied

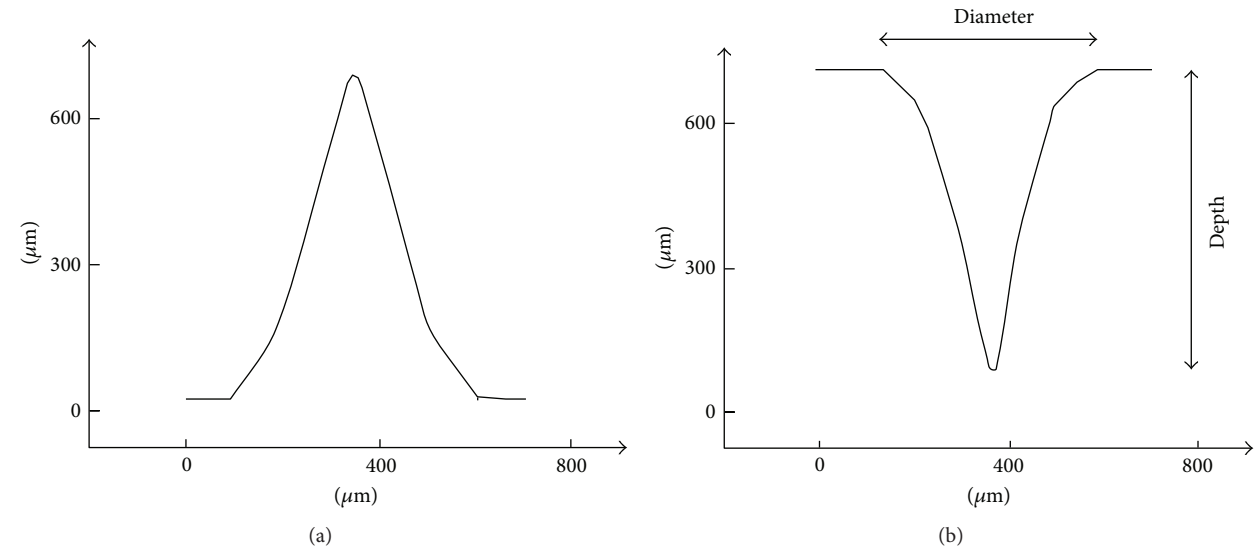

Figure 6: Two-dimensional profiles for (a) the conical pillar on the imprinting mold and (b) the microhole on the nanocomposite imprinted at 500 kg, measured by the confocal laser scanning microscopy.

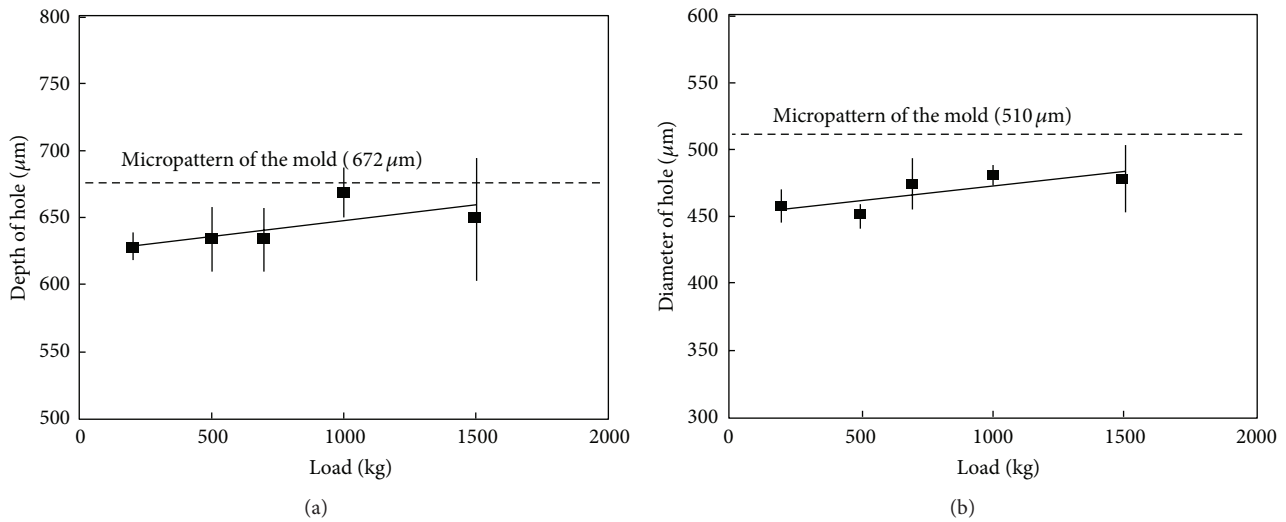

Figure 7: Dependence of the imprinting load on the fabricated hole (a) depth and (b) diameter of the SiO_2-PVA nanocomposites, measured by the confocal laser scanning microscopy. The broken lines in the figure indicate height or diameter of the micropatterns for the imprinting mold.

that plastic deformation of the nanocomposites takes place on the order of submillimeter dimensions even at room temperature. To optimize the imprinting load, hole diameter and depth were measured as a function of the load. Figure 7 shows hole depth and diameter of the fabricated micropatterns on the nanocomposites by the room temperature imprint as a function of the load. Both the hole depth and diameter for the nanocomposites increased with increasing load and then approach those values for the imprinting mold. However, in the cases which exceed 700 kg of load, there were signs of macrocrack formation at the corner of the nanocomposites during the room temperature imprint, as shown in Figure 8. Therefore, the optimal load was considered to be ~500 kg.

After the imprinting, the monolithic SiO_2-PVA nanocomposite was sintered at 1200°C in air to form the silica glass. During the sintering process, the PVA moiety of the nanocomposites was decomposed; subsequently the silica nanoparticles were mutually sintered to diminish the mesopores. Consequently, transparent and dense silica glass was obtained. Figures 9(a) and 9(b) show the sintered silica glass and the fabricated micropatterns on the surface. Table 2 lists the fabricated dimensions of the micropatterns before

Figure 8: Photograph of the imprinted SiO_2-PVA nanocomposites with variation of imprinting load. The arrows indicate the macrocracks.

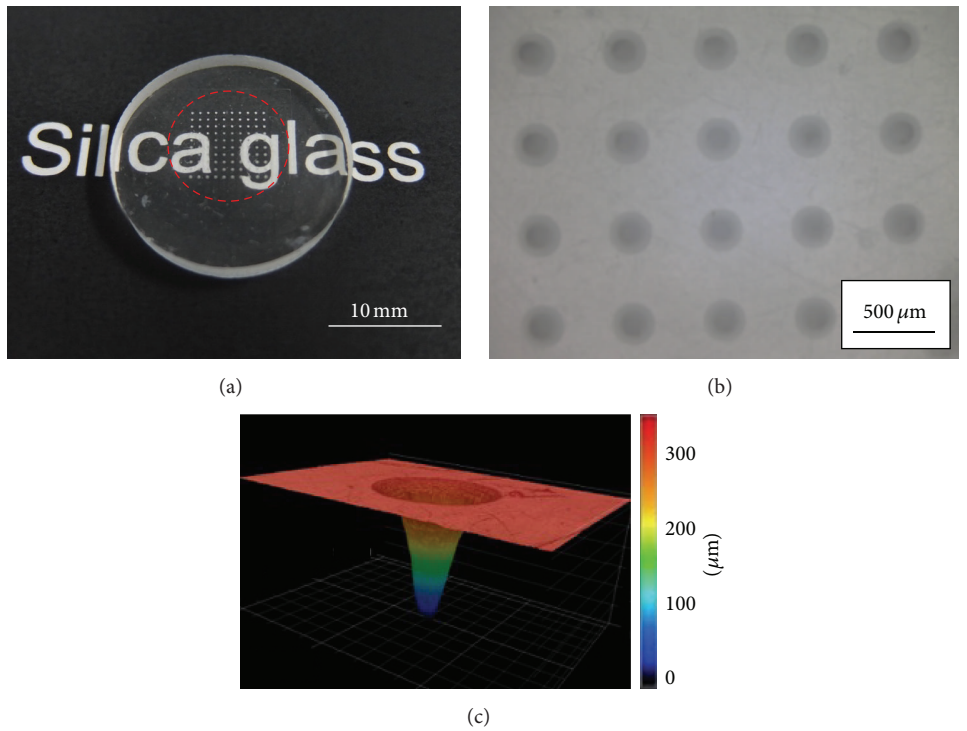

Figure 9: (a) Photograph of the sintered silica glass possessing the micro-conical-hole array on the surface (the broken circle indicates the micropatterned area), (b) the microhole array on the silica glass as observed by a microscope, and (c) three-dimensional image for the micro-conical-hole on the sintered silica glass measured by the confocal laser scanning microscopy.

Table 1: BET specific surface area, total pore volume, and mean pore diameter of the SiO_2-PVA nanocomposites prepared from 7 and 30 nm silica particles via an SiO_2-PVA suspension as a function of pH.

pH value of suspension	BET surface area/$m^2\ g^{-1}$	Total pore volume/$cm^3\ g^{-1}$	Mean pore radius/nm
Aerosil 300 (mean diameter of 7 nm)			
2.3	147	1.08	14.7
3.0	141	0.95	13.5
3.4	142	0.94	13.2
4.0	146	0.93	12.7
4.7	144	0.89	12.4
Aerosil 50 (mean diameter of 30 nm)			
2.3	32	0.15	9.6
3.1	31	0.08	5.2
3.3	31	0.10	6.6
5.0	32	0.11	6.8

(nanocomposite) and after (silica glass) sintering. Although the micropatterns of the silica glass reduced by half as a result of the sintering, the aspect ratio for the micropatterns of the silica glass remained constant in comparison to the dimensions of the imprinting mold. Figure 9(c) suggests that the fabricated microhole on the silica glass possessed a conical shape.

From these results, we conclude that the micro-conical-hole array can be fabricated on the silica glass via room temperature imprint using the crack-free monolithic SiO_2-PVA nanocomposite as the silica glass precursor. This is in contrast to the present methods, whereby challenges remain with respect to fabricating micropattern arrays by conventional processes, such as semiconductor lithography techniques, mechanical processing, and thermal imprint. Therefore, the present method described herein is considered to be an attractive alternative for fabricating microperiodic

Table 2: Micropattern dimensions of the imprinting mold, the imprinted nanocomposite, and the sintered silica glass.

	Depth (or height)/μm	Diameter/μm	Aspect ratio (depth/diameter)
Imprinting mold	672 ± 3	510 ± 2	1.3
Nanocomposite (before sintering)	634 ± 24	450 ± 9	1.4
Silica glass (after sintering)	342 ± 18	263 ± 7	1.3

structures onto silica glass for multiple functional devices. To repeatedly fabricate additional complicated microstructures precisely by the room temperature imprint, the viscoelastic properties and deformation mechanism of the SiO_2-PVA nanocomposite are currently under further investigation.

4. Conclusions

Monolithic and crack-free mesoporous SiO_2-PVA nanocomposite has been prepared by fumed silica nanoparticles via an SiO_2-PVA suspension at pH 3. Micropatterns were fabricated onto the nanocomposites by imprinting at room temperature with 500 kg of load. The nanocomposites were sintered at 1200°C in air, consequently forming transparent silica glasses possessing micro-conical-hole array representative of the mold shape and dimension.

Conflict of Interests

The authors declare that there is no conflict of interests regarding the publication of this paper.

Acknowledgments

This work was supported by JSPS KAKENHI Grant no. 26420756. The authors also acknowledge the funding from the Promote Business Creation Project Based on Growth Strategy of Kyusyu, Japan, 2013. The authors would like to thank WORKS Co., Ltd., for experimental support.

References

[1] H. Ito, M. Arai, Y. Matsui, and D. Itagaki, "Experimental testing and FEM simulation for thermal imprinting of micro/nano glass-optical devices," *Journal of Non-Crystalline Solids*, vol. 362, no. 1, pp. 246–254, 2013.

[2] H. Mekaru, T. Tsuchida, J.-I. Uegaki, M. Yasui, M. Yamashita, and M. Takahashi, "Micro lens imprinted on Pyrex glass by using amorphous Ni-P alloy mold," *Microelectronic Engineering*, vol. 85, no. 5-6, pp. 873–876, 2008.

[3] T. Mori, K. Hasegawa, T. Hatano, H. Kasa, K. Kintaka, and J. Nishii, "Surface-relief gratings with high spatial frequency fabricated using direct glass imprinting process," *Optics Letters*, vol. 33, no. 5, pp. 428–430, 2008.

[4] I. Yamada, N. Yamashita, K. Tani et al., "Fabrication of achromatic infrared wave plate by direct imprinting process on chalcogenide glass," *Applied Physics Express*, vol. 5, no. 7, Article ID 072601, 2012.

[5] T. Tamura, M. Umetani, K. Yamada et al., "Fabrication of antireflective subwavelength structure on spherical glass surface using imprinting process," *Applied Physics Express*, vol. 3, no. 11, Article ID 112501, 2010.

[6] T. Han, S. Madden, D. Bulla, and B. Luther-Davies, "Low loss chalcogenide glass waveguides by thermal nano-imprint lithography," *Optics Express*, vol. 18, no. 18, pp. 19286–19291, 2010.

[7] Q. Chen, Q. Chen, and G. MacCioni, "Fabrication of microfluidics structures on different glasses by simplified imprinting technique," *Current Applied Physics*, vol. 13, no. 1, pp. 256–261, 2013.

[8] Q. Chen, Q. Chen, D. Milanese, and M. Ferraris, "Microstructures fabrication on glasses for micro-fluidics by imprinting technique," *Microsystem Technologies-Micro-and Nanosystems-Information Storage and Processing Systems*, vol. 15, no. 7, pp. 1067–1071, 2009.

[9] H. Takebe, M. Kuwabara, M. Komori, N. Fukugami, M. Soma, and T. Kusuura, "Imprinted optical pattern of low-softening phosphate glass," *Optics Letters*, vol. 32, no. 18, pp. 2750–2752, 2007.

[10] N. Kobayashi, T. Mori, T. Suetsugu et al., "Fabrication of glasses with low softening temperatures for mold-processing by ion-exchange," *Journal of the Ceramic Society of Japan*, vol. 116, no. 1356, pp. 875–879, 2008.

[11] I. Yamada, N. Yamashita, T. Einishi, M. Saito, K. Fukumi, and J. Nishii, "Design and fabrication of an achromatic infrared wave plate with Sb-Ge-Sn-S system chalcogenide glass," *Applied Optics*, vol. 52, no. 7, pp. 1377–1382, 2013.

[12] M. Takahashi, K. Sugimoto, and R. Maeda, "Nanoimprint of glass materials with glassy carbon molds fabricated by focused-ion-beam etching," *Japanese Journal of Applied Physics, Part 1: Regular Papers and Short Notes and Review Papers*, vol. 44, no. 7, pp. 5600–5605, 2005.

[13] H. Ikeda, S. Fujino, and T. Kajiwara, "Fabrication of micropatterns on silica glass by a room-temperature imprinting method," *Journal of the American Ceramic Society*, vol. 94, no. 8, pp. 2319–2322, 2011.

[14] E. P. Barrett, L. G. Joyner, and P. P. Halenda, "The determination of pore volume and area distributions in porous substances. I. Computations from nitrogen isotherms," *Journal of the American Chemical Society*, vol. 73, no. 1, pp. 373–380, 1951.

[15] S. Brunauer, P. H. Emmett, and E. Teller, "Adsorption of gases in multimolecular layers," *Journal of the American Chemical Society*, vol. 60, no. 2, pp. 309–319, 1938.

[16] H. Ikeda and S. Fujino, "Composition and pH dependence on aggregation of SiO_2–PVA suspension for the synthesis of porous SiO_2–PVA nanocomposite," *Journal of Porous Materials*, vol. 21, no. 6, pp. 1143–1149, 2014.

[17] F. Kirkbir, H. Murata, D. Meyers, S. R. Chaudhuri, and A. Sarkar, "Drying and sintering of sol-gel derived large SiO_2 monoliths," *Journal of Sol-Gel Science and Technology*, vol. 6, no. 3, pp. 203–217, 1996.